Genetic requirement for *Esrp1/2* in vertebrate pituitary morphogenesis

Running title: *Esrp1/2* in pituitary morphogenesis

Shannon H. Carroll[1,2], Sogand Schafer[1], Ariella S. Richman[1], Lisa Tsay[1], Peng Wang[3], Mian Umair Ahsan[3], Kai Wang[3,4] and Eric C. Liao[1,2*]

[1]Center for Craniofacial Innovation, Division of Plastic and Reconstructive Surgery, Department of Surgery, Children's Hospital of Philadelphia, Philadelphia, PA, USA.

[2]Shriners Hospital for Children, Tampa, FL, USA.

[3]Center for Cellular and Molecular Therapeutics, Children's Hospital of Philadelphia, Philadelphia, PA, USA.

[4]Department of Pathology and Laboratory Medicine, University of Pennsylvania, Philadelphia, PA, USA.

[*]Author for correspondence: liaoce@chop.edu

Keywords: *ESRP1*, *ESRP2,* cleft palate, pituitary, adenohypophysis

Abstract

The pituitary gland produces several hormones that regulate growth, metabolism, stress response, reproduction, and homeostasis. Congenital hypopituitarism is a deficiency in one or more pituitary hormones and encompasses a spectrum of clinical conditions. The pituitary has a complex embryonic origin with the oral ectoderm contributing the anterior lobe, and the neural ectoderm generating the posterior lobe. Pituitary abnormalities and growth deficiencies are associated with cleft palate however the developmental genetic connection between pituitary and orofacial cleft malformations remains to be determined. The epithelial RNA splicing regulators *Esrp1* and *Esrp2* are required for orofacial development in zebrafish, mice, and humans, and loss of function of these genes results in a cleft palate. Here we present a detailed developmental analysis of the genetic requirement for *Esrp1/2* in pituitary morphogenesis in mouse and zebrafish. Further, we describe a patient with cleft palate and hypopituitarism that harbors a nucleotide variant in the RNA binding domain of *ESRP2*. The discovery of this key function for *Esrp1/2* in pituitary formation has significant fundamental and clinical implications for understanding congenital hypopituitarism and craniofacial anomalies.

Summary Statement

Esrp1 and Esrp2 are regulators of mRNA alternative splicing that are required for both orofacial and pituitary development in vertebrates.

Introduction

The pituitary gland is a midline structure that resides in the sella turcica recess of the sphenoid bone at the base of the brain. The pituitary has a complex embryonic origin with the oral ectoderm contributing the anterior lobe, the neural ectoderm generating the posterior lobe, and a recently identified contribution from the endoderm (Fabian et al., 2020; McCabe and Dattani, 2014). The pituitary gland produces several hormones with essential systemic physiologic effects in maintaining growth, metabolism, stress response, reproduction, and homeostasis (McCabe and Dattani, 2014; Prodam et al., 2021; Rizzoti and Lovell-Badge, 2005). Congenital hypopituitarism (CH) is defined as a deficiency in one or more pituitary hormones and encompasses a spectrum of clinical conditions with both familial and sporadic occurrences (Higham et al., 2016; McCabe and Dattani, 2014; Prodam et al., 2021). Non-specific symptoms may present in neonates. However, the full clinical sequalae of central pituitary deficiencies may not present until adolescence or young adulthood (Higham et al., 2016).

Midline craniofacial defects including holoprosencephaly (HPE) and septo-optic dysplasia (SOD), are often associated with pituitary deficiency (McCabe and Dattani, 2014; Prodam et al., 2021). Pituitary abnormalities and growth deficiencies are also associated with isolated cleft palate (Akin et al., 2014; Bowers et al., 1988; Laron et al., 1969; Roitman and Laron, 1978; Rudman et al., 1978), a common birth defect occurring in approximately 1 in 700 births (Dixon et al., 2011). The developmental genetic connection between pituitary and orofacial cleft malformations remains to be determined.

We and others have shown that the epithelial RNA splicing regulators *Esrp1* and *Esrp2* are required for orofacial development in zebrafish, mice, and humans (Bebee et al., 2015; Burguera et al., 2017; Carroll et al., 2020). Ablation of *esrp1* and *esrp2* in zebrafish results in several developmental defects, including a cleft that involves the upper mouth opening and the anterior neurocranium (ANC) (Burguera et al., 2017; Carroll et al., 2020), a structure with embryonic similarity to the mammalian primary palate (Carroll et al., 2020). In the mouse, ablation of *Esrp1* causes a bilateral cleft lip and cleft palate, and ablation of both *Esrp1* and *Esrp2* leads to a more severe bilateral cleft lip and palate phenotype (Bebee et al., 2015; Carroll et al., 2020; Lee et al., 2020). Finally, *ESRP2* human gene variants have been found in cleft lip and palate clinical cohorts, whereas so far *ESRP1* gene variants have been associated with hearing deficits (Cox et al., 2018; Rohacek et al., 2017).

Across zebrafish and mouse, we found that *Esrp1* and *Esrp2* transcripts are co-localized in epithelial cells throughout early embryonic development, including in the surface and oral epithelium (Carroll et al., 2020). Since the oropharyngeal epithelium contributes to anterior pituitary development, we hypothesized that pituitary development may be disrupted in *Esrp1/2* null murine and zebrafish models. Herein we present a detailed developmental analysis of *Esrp1/2* in mouse and zebrafish revealing the genetic requirement for *Esrp1/2* in pituitary morphogenesis. Given the key role of *Esrp1/2 in* generating specific isoforms of its target genes that regulate epithelial function, the discovery of this key role for *Esrp1/2* in pituitary formation has significant fundamental and clinical implications for understanding CH and craniofacial anomalies.

Results

Esrp1 and *Esrp2* transcripts are detected in Rathke's pouch and the anterior and intermediate pituitary

We described previously that *Esrp1* and *Esrp2* genes are expressed within the oral epithelium of mouse embryos (Carroll et al., 2020). Prior work has shown that the mammalian anterior and intermediate pituitary develop through an invagination of the oral epithelium, termed Rathke's pouch. We analyzed *Esrp1* and *Esrp2* expression during key time points of mouse pituitary morphogenesis. At E10.25, *Esrp1* and *Esrp2* transcripts were co-localized in the epithelial cells lining the cranial structures, including the invaginating epithelium that will go on to form Rathke's pouch (Fig.1 A). No *Esrp1/2* gene expression was detected within the neuroectoderm. At E11.5 and E12.5 *Esrp1* and *Esrp2* were co-localized in the enclosed epithelium, forming Rathke's pouch (Fig.1 B and C, respectively). *Esrp1* and *Esrp2* gene expressions persisted in the mature pituitary gland (P0) (Fig. 1 D). The expression of *Esrp1/2* across the span of pituitary morphogenesis suggested a potential role in morphogenesis.

Anterior pituitary failed to develop in *Esrp1/2* null mice

Prior work showed that *Esrp1* null and *Esrp1/2* compound null mice exhibit bilateral cleft lip and cleft palate and neonates die shortly after birth (Bebee et al., 2015; Carroll et al., 2020; Lee et al., 2020). To investigate the role of *Esrp1/2* in pituitary morphogenesis we collected pups from *Esrp1+/-; Esrp2+/-* breeding in-crosses. Histological examination of the pituitary gland and surrounding structures at P0 and E17.5 revealed that *Esrp1-/-; Esrp2-/-* compound null mice exhibited severely

hypoplastic or absent anterior pituitary (Fig. 2 and Fig. S1A, respectively). We observed a similar phenotype in *Esrp1-/-*; *Esrp2*+/+ pups at E17.5, where the anterior pituitary was absent (Fig. S1B). *As Esrp1+/+; Esrp2-/-* mice grow and reproduce normally, we did not analyze pituitary development in the *Esrp2* nulls. The intermediate pituitary of *Esrp1-/-; Esrp2-/-* null mice is dysmorphic whereas the posterior pituitary is intact, though somewhat hypoplastic (Fig. 2). We confirmed that *Esrp1-/-; Esrp2-/-* null mice have a present, though dysmorphic, intermediate pituitary by staining for *Sox2* gene expression which is highly enriched in intermediate pituitary cells (Cheung et al., 2017) (Fig. 2B). Growth hormone (*GH*) is expressed in the anterior pituitary and was absent in the *Esrp1-/-; Esrp2-/-* null mice (Fig. 2B). *POMC* is expressed in the intermediate and anterior pituitary and was observed to be present but diminished in the *Esrp1-/-; Esrp2-/-* null mice (Fig. 2B). Taken together, these results indicate an absence of an anterior pituitary in *Esrp1-/-; Esrp2-/-* null mice, as well as the absence of functional anterior pituitary endocrine cells.

To determine the stage at which anterior pituitary development becomes disrupted in the *Esrp1-/-; Esrp2-/-* null mice, histology was performed at various time points. At E12.5, control embryos have a fully formed Rathke's pouch that has begun to separate from the oral epithelium (Fig.3, Fig. S2). In *Esrp1-/-; Esrp2-/-* null littermates, Rathke's pouch has invaginated and closed however the closure of the pouch is abnormal, and the resulting structure is dysmorphic and hypoplastic (Fig. 3, Fig. S2). The presence of *Lhx3* and *Prop1* mRNA in Rathke's pouch of *Esrp1-/-; Esrp2-/-* null mice suggested that the specification of pituitary progenitor cells was preserved, but subsequent proliferation and contribution of these cells to form the Rathke's pouch and

anterior pituitary were defective (de Moraes et al., 2012; Gregory and Dattani, 2020; Perez Millan et al., 2024) (Fig. 3, Fig. S2).

Invagination of the oral epithelium and formation of Rathke's pouch relies on a series of signaling pathways and morphogens that are spatially restricted (de Moraes et al., 2012; Rizzoti and Lovell-Badge, 2005; Takuma et al., 1998; Treier et al., 1998; Zhu et al., 2007). One important signal for the invagination of the epithelium is Fgf secreted from the adjacent neuroectoderm (Ericson et al., 1998; Norlin et al., 2000; Treier et al., 1998). *Esrp1/2* are known to regulate the alternative splicing of Fgf receptors and are required for the expression of the epithelial *Fgfr1IIIb* isoform (Bebee et al., 2015). To test whether loss of *Esrp1/2* affects *Fgfr1* isoform expression in the invaginating epithelium forming Rathke's pouch, we performed Basescope isoform-specific *in situ* hybridization in E10.5 *Esrp1-/-;Esrp2-/-* null and littermate control mouse embryos. Already at E10.5, *Esrp1-/; Esrp2-/-* null mice have a smaller area of invaginated epithelium that is shallower than in control littermates (Fig 4). Further, *Esrp1-/-; Esrp2-/-* null mice have fewer cells exhibiting a columnar and stratified morphology, as in the littermate controls. The presence of *Fgfr1IIIb* and *Fgfr1IIIc* isoform transcripts were quantified by counting the number of individual RNAscope signals detected within the invaginated epithelium. *Esrp1-/-; Esrp2-/-* null mice had lower total expression of *Fgfr1IIIb* isoform as well as a lower number of isoform transcripts per cell (Fig. 4). These data show that *Esrp1/2* regulates the *Fgfr1* epithelial isoform expression within the epithelium contributing Rathke's pouch. However, how changes to *Fgfr1* isoform expression affect Rathke's pouch formation remains to be determined.

esrp1 and _esrp2_ genes are expressed in the zebrafish adenohypophyseal placode and developing pituitary

It has been previously described that zebrafish compound mutants for *esrp1* and *esrp2* have abnormal craniofacial development (Burguera et al., 2017; Carroll et al., 2020). The upper margin of the mouth of *esrp1/2* mutant zebrafish is discontinuous and the anterior neurocranium exhibits a cleft in the median portion which is populated by an aberrant cluster of cells (Burguera et al., 2017; Carroll et al., 2020). These findings in zebrafish mutants corroborate that the developmental processes of orofacial cleft pathogenesis, with regard to the anterior structures such as the mouth opening and primary palate, are similar between zebrafish and amniotes.

Given the commonalities of the craniofacial phenotypes in *Esrp1/2* null mice and zebrafish, as well as the dysmorphic Rathke's pouch and hypoplastic anterior pituitary lobe observed in the *Esrp1-/-,Esrp2-/-* null mice, we examined pituitary morphogenesis in the *esrp1/2* mutant zebrafish. We first characterized *esrp1* and *esrp2* expression in the developing adenohypophysis (ADH) of zebrafish embryos. At 24 hours post-fertilization (hpf), the adenohypophyseal placode has specified at the rostral-most midline of the embryo and is identified by *pitx3* expression (Dutta et al., 2005; Zilinski et al., 2005). *esrp1* was highly expressed within these *pitx3*-expressing cells (Fig. 5A). At 27 hpf the cells of the adenohypophyseal placode have begun moving caudally (Fig. 5B). At this early stage of development, presumptive adenohypophyseal and hypothalamic cells express proopiomelanocortin a (*pomca*) (Fig.5B). *esrp1* transcripts were detected within *pomca*-expressing adenohypophyseal cells, and cells of the

developing oral epithelium (Fig. 5B). Therefore, similarly to mouse, *esrp1/2* are expressed in the developing pituitary across morphogenesis.

esrp1/2 are required for zebrafish adenohypopyseal morphologenesis

To examine whether adenohypophysis development is disrupted in *esrp1/2* mutant zebrafish, whole-mount RNA *in situ* hybridization was performed for key genes that function in the pituitary; *pomca*, prolactin (*prl*), and growth hormone (*gh*) in *esrp1/2* mutant and clutch-mate controls at 3 days post-fertilization (dpf). Interestingly, in the *esrp1/2* mutants, cells marked with *pomca*, *prl,* and *gh* transcripts were displaced ventro-rostrally relative to controls. *pomca* gene expression was particularly aberrant in *esrp1/2* mutants relative to controls, as *pomca* positive cells were found to be lining the oral cavity, including the lower jaw element (Fig. 6A). Using RNAscope whole-mount RNA *in situ* hybridization we obtained similar results for *pomca* expression. *esrp1/2* mutants have similar hypothalamic expression of *pomca* relative to controls, but there is also high level of expression within the mouth (Fig. 6B). Further, the expression pattern of *pomca* in the *esrp1/2* mutant mouths also varied more between individuals, in contrast to wildtype where the localization of *pomca* expression was consistent at the skull base (Fig. 6B).

To obtain cellular resolution of pituitary cells in control versus *esrp1/2* mutant zebrafish we performed RNAscope *in situ* hybridization on sagittal sections obtained at the midline at 3 dpf. We used keratin 4 (*krt4*) expression to identify embryonic epithelium and *lhx3* and *pitx3* gene expressions to define the adenohypophysis. Consistent with whole-mount imaging, we found that *lhx3* and *pitx3* transcripts were

present in *esrp1/2* mutants but ectopically localized to a ventro-rostral position, suggesting a lack of transit to a more dorsal and caudal location where the pituitary would reside (Fig. 6C). *prl* and *pomca* were detected in the ectopically localized cells (Fig. 6C), which is analogous to the observation in the mouse that the pituitary progenitors are specified but fail to localize and contribute the anterior pituitary. Taken together, we show that the adenohypophysis of *esrp1/2* mutant zebrafish forms aberrantly, with pituitary progenitors failing to reach their proper location, though differentiation is unaffected.

In situ hybridization results suggest impaired translocation of the pituitary anlage in *esrp1/2* mutants. To visualize pituitary development in real-time, we generated a zebrafish pituitary reporter line by inserting tdTomato into the first exon of *lhx3* (Fig. 7A). In zebrafish, *lhx3* is one of the first genes expressed in the adenohypophyseal placode and pituitary anlage and is highly tissue-specific at the developmental time points of interest (Glasgow et al., 1997; Herzog et al., 2003). Light-sheet microscopic imaging of live zebrafish wildtype embryos from 27-42 hpf shows translocation of *lhx3* positive cells from a position just superficial to the surface ectoderm near the future stomodeum to a ventral and more caudal position (Fig. 7B,C, Movies 1-4). The *lhx3*-expressing cells of the pituitary anlage also express *cdh1*, as was shown previously (Fabian et al., 2020).

We utilized our newly generated *lhx3*:tdTomato reporter line to visualize the developing pituitary in the *esrp1/2* mutant zebrafish. As *esrp1/2* mutants are visually identifiable starting at 48 hpf, we imaged mutants and wildtype clutch-mate controls at 48 and 72 hpf. Similar to our *in situ hybridization* results, we found that the *lhx3* positive pituitary of *esrp1/2* mutants failed to translocate to the proper position and that *lhx3*

expression was expressed exogenously in the oral cavity just superficial to the abnormal ANC (Fig. 7D,E).

A single nucleotide variant in *ESRP2* associated with cleft palate and hypopituitarism

Our finding of anterior pituitary dysmorphogenesis in *Esrp1/2* null mice and zebrafish, which also display cleft of the lip and palate, supports an etiological link between orofacial clefts and congenital hypopituitarism that has been previously proposed (Akin et al., 2014; Bowers et al., 1988; Laron et al., 1969; McCabe and Dattani, 2014; Prodam et al., 2021; Roitman and Laron, 1978; Rudman et al., 1978). To assay whether *ESRP2*, which has been previously reported to be associated with orofacial clefts (Cox et al., 2018; Rohacek et al., 2017), is also associated with congenital hypopituitarism, we analyzed clinical and genomic data in the Arcus database from the Children's Hospital of Philadelphia. The Arcus database contains whole exome sequencing data from 6,903 patients undergoing clinical exome sequencing testing for a variety of clinical conditions. Of these, we identified 8 patients with both congenital hypopituitarism and orofacial cleft. In one patient, we identified a nonsynonymous single nucleotide variant (SNV) (16-68232468-C-T in GRCh38 coordinate) in *ESRP2* that results in an arginine-to-histidine amino acid change (p.R286H) in the coding region of exon 8 based on MANE select transcript NM_024939.3 (Fig. 8A,B). This amino acid is conserved across species (Fig. 8C). This SNV is located in the RNA recognition motif domain, and it is predicted to be deleterious by the dbNSFP database (for example, it has an AlphaMissense score of 0.95 and a

MetaRNN score of 0.85) (Liu et al., 2020). It has a population maximum frequency of 0.0000147 in the gnomAD version 4.1 database (Karczewski et al., 2020), indicating that it is extremely rare. To examine whether there is another stronger candidate in the individual that explains the cleft palate, we examined the 418 previously known genes associated with orofacial cleft (Caetano da Silva et al., 2024) plus ESRP1 gene in this patient. However, we did not find another variant that is predicted to be deleterious or reported to be pathogenic in the ClinVar database (Landrum et al., 2014). Moreover, this *ESRP2* variant was predicted to be the most deleterious SNV based on dbNSFP database among all variants in the 419 genes. The known pathogenic variants reported in ClinVar for this patient were also examined. There are three known pathogenic variants from PERM1 (ClinVar Variation ID: 1320032), ITPKB (ClinVar Variation ID: 1705896), and SORD (ClinVar Variation ID: 929258) respectively. All these three variants were not able to explain the phenotype of pituitary deficiency and orofacial clefts. Therefore, the *ESRP2* variant remains the most likely pathogenic variant in this individual that explains both pituitary abnormality and orofacial cleft.

Discussion

Development of the mammalian pituitary gland requires an interaction between closely associated ectodermal tissue, namely the surface/oral ectoderm and the neuroectoderm. Molecular signaling between these tissues must be spatially and temporally restricted and coordinated such that specific alterations in ectoderm morphology are produced, resulting in the surface/oral ectoderm-derived anterior lobe and the neuroectoderm-derived posterior lobe. The events leading to pituitary organogenesis in zebrafish are less clear however several morphogens and growth factors have been shown to be conserved (Herzog et al., 2004; Herzog et al., 2003; Pogoda and Hammerschmidt, 2007).

Here we demonstrate that *Esrp1/2* are required for the early events of pituitary organogenesis in both mice and zebrafish. Early during surface/oral ectoderm invagination, *Esrp1-/-;Esrp2-/-* mouse embryos demonstrate a more shallow invagination and abnormal cellular morphology of Rathke's pouch. The resulting Rathke's pouch of *Esrp1-/-;Esrp2-/-* mouse embryos is hypoplastic and improperly formed. Invagination of the surface/oral ectoderm is initiated and supported by Bmp4 and Fgf8/10 signals emanating from the adjacent infundibulum (Takuma et al., 1998). *Esrp1/2* are expressed in the surface/oral ectoderm and are known regulators of Fgf receptors where the loss of *Esrp1/2* results in decreased expression of the *IIIb* receptor isoform of *Fgfr1*, *Fgfr2*, and *Fgfr3*. This is also true in the invaginating prospective Rathke's pouch, as *Esrp1-/-; Esrp2-/-* embryos had decreased expression of the *Fgfr1IIIb* isoform. The functional significance of *IIIb* versus *IIIc* isoform expression remains unknown, though these isoforms contain different domains that likely change

ligand/receptor kinetics. That reduced expression of *Fgfr1IIIb* in *Esrp1-/-; Esrp2-/-* embryos may lead to improper Rathke's pouch formation is supported by the previous finding that mice with specific ablation of the *Fgfr2IIIb* isoform have abnormal surface/oral ectoderm invagination and a failure to form a definitive pouch (De Moerlooze et al., 2000).

Importantly, this improper morphogenesis of Rathke's pouch in *Esrp1-/-; Esrp2-/-* embryos is independent of pituitary cell specification as early pituitary-dependent transcription factors are normally expressed. Interestingly, these pituitary progenitors do not go on to produce hormone-expressing cells, as these differentiated cells are absent in the mature anterior pituitary. The formation of the anterior lobe occurs through an epithelial-to-mesenchymal (EMT)-like transition of epithelial cells of the lumen of Rathke's cleft where the cells differentiate, delaminate, and migrate, and contribute the parenchyma of the anterior lobe (Cheung et al., 2017). Esrp1/2 exert an epithelial-specific splicing program that is reverted upon initiation of EMT (Warzecha et al., 2010; Yang et al., 2016) and Esrp1/2 are implicated in developmental processes, organogenesis, as well as cancer progression (Derham and Kalsotra, 2023). It is possible that an improper splicing program in lumen epithelial cells of the *Esrp1/2* null embryos impairs the EMT-like transition necessary for the development of the anterior lobe. It is alternatively possible that the loss of an anterior lobe in the *Esrp1/2* null embryos is due to dysregulated proliferation or apoptosis of the migratory cells. In *Fgfr2IIIb* null mice, upregulated apoptosis was found in the newly formed anterior parenchyma, which may have led to the lack of an anterior lobe in these mice (De Moerlooze et al., 2000).

The embryonic development of the zebrafish pituitary (or adenohypohysis) is thought to be significantly different from that of amniotes in that zebrafish pituitary morphogenesis begins with the internalization of the superficial adenohypophyseal placode, and there is no obvious equivalent to Rathke's pouch. Additionally, cells of the internalizing anlage already express the hormones *prolactin* and *pomc,* suggesting terminal differentiation of lactotropes and corticotropes before organogenesis is completed (Herzog et al., 2003; Pogoda and Hammerschmidt, 2007). However, It has also been postulated that the invagination of the zebrafish stomodeum, which occurs in concert with the repositioning of the pituitary anlage represents a morphogenic equivalent between teleost and mammalian Rathke's pouch (Fabian et al., 2020; Herzog et al., 2003). This hypothesis has yet to be tested. Here, we demonstrate a shared requirement for *Esrp1/2* during pituitary morphogenesis in the mouse and zebrafish. This finding supports a conserved cellular mechanism for pituitary morphogenesis across these species.

A number of genes that are causative of congenital hypopituitarism (CH) have been identified, however, these account for less than 25% of cases (Camper et al., 2023; Fang et al., 2016). The novel identification of *Esrp1/2* as a regulator of pituitary morphogenesis identifies it as a new gene candidate for the genetic diagnosis of CH. Genomic analysis using the known causative genes of CH failed to assign a genetic diagnosis for the patient described in this study. Our identification of a deleterious SNV in ESRP2 in this patient suggests that ESRP2 may be a new CH gene candidate. Functional testing of this specific variant in animal models, as well as additional analysis with larger CH cohorts, are needed to assign a causal link between CH and *ESRP2*.

Further, targets of Esrp1/2 RNA regulation and splicing are promising candidates for being causative of CH. The consideration of alternatively spliced variants, and the utilization of transcriptome data for CH genetic diagnoses, has recently been highlighted (Camper et al., 2023). Our discovery of the requirement of *Esrp1/2* for pituitary morphogenesis across vertebrates underscores the developmental and clinical importance of alternative splicing.

Materials and Methods

Animals

All animal experiments were performed in accordance with protocols approved by Children's Hospital of Philadelphia Institutional Animal Care and Use Committee. C57Bl/6J (WT) mice (*Mus musculus*) were obtained from the Jackson Laboratory. *Esrp1*$^{+/-}$; *Esrp2*$^{-/-}$ mice were received from Dr. Russ Carstens. Embryonic day 0.5 was considered to be noon on the day of the copulatory plug.

Zebrafish (*Danio rerio*) adults and embryos were maintained in accordance with approved institutional protocols at Children's Hospital of Philadelphia. Embryos were raised at 28.5°C in E3 medium (5.0 mM NaCl, 0.17 mM KCl, 0.33 mM $CaCl_2$, 0.33 mM $MgSO_4$) with 0.0001% methylene blue. Embryos were staged according to standardized developmental time points by hours or days post-fertilization (hpf or dpf, respectively). All zebrafish lines used for experimentation were generated from the Tübingen strain. The *esrp1* and *esrp2* CRISPR mutants were generated as previously described (Carroll et al., 2020). The *lhx3*:tdTomato reporter line was generated using a previously described protocol(Auer et al., 2014; Hawkins et al., 2021). Briefly, a CRISPR guide targeting exon one near the ATG of *lhx3* was designed using Integrated DNA Technologies' Custom Alt-R CRISPR Cas9 guide RNA design tool. The donor plasmid containing the tdTomato sequence, an HSP70 promoter, and a linearization cut site was gifted by Dr. Matt Harris. The guide, donor plasmid, plasmid linearization guide, lhx3-targeting guide, and Cas9 protein were injected into 1-cell stage zebrafish embryos. Proper insertion of the tdTomato donor DNA was determined by screening for heat shock-induced tdTomato expression followed by Sanger sequencing.

Whole-mount *in situ* hybridization

Embryos were isolated at various time points and fixed in 4% formaldehyde at 4°C for 12-16 hrs. Subsequently, embryos were washed and stored in methanol. WISH and DIG-labeled riboprobes were synthesized as described (Thisse and Thisse, 2008). WISH colorimetric signal detection was performed using an alkaline phosphatase-conjugated anti-DIG antibody (Roche) and BM Purple AP substrate (Roche).

RNAscope and Basescope *in situ* hybridization

Zebrafish and mouse embryos were fixed in 4% formaldehyde, taken through a sucrose gradient and cryo-embedded and sectioned. Probes were designed and purchased from ACD Bio, and hybridization and staining were performed according to the manufacturer's protocol. For whole-mount RNAscope *in situ* hybridization, zebrafish embryos were processed as described (Gross-Thebing et al., 2014) and imaged in 0.2% low-melt agarose. Whole-mounts and stained sections were imaged using a confocal microscope, where a z-stack was obtained and analyzed on ImageJ for z-stack maximum intensity projections. For Basescope, probes were designed and purchased from ACD Bio. Serial sagittal cryosections were taken through the mouse embryo heads and sections, where Rathke's pouch was most invaginated, were chosen for Basescope *in situ* hybridization. Hybridization and staining were performed according to the manufacturer's protocol. Stained sections were imaged with a Leica brightfield microscope. To quantify expression, the entire invaginated epithelium on a single section was manually identified, and the total number of green dots and red dots was

counted. As the invaginated area of *Esrp1/2* -/- mice were smaller than littermate controls, the total number of cells was counted and used to normalize the transcript number.

Clinical genomic data analysis

To examine patients with pathogenic or likely pathogenic ESRP1/ESRP2 mutations in CHOP patients, we examined de-identified clinical records on a set of ~6900 patients affected with a range of clinical conditions with paired clinical exome sequencing results from the Division of Genomic Diagnostics (DGD). This analysis was performed in the institutional computing platform called Arcus, where clinical records and genome/exome sequencing data are available on subjects. We examined patients with Cleft Palate (CP, icd10 code - Q35) and Hypopituitarism (HPP, icd10 code - E23) annotations. The functional analysis of the variants and patient's whole exome sequencing (in VCF format) was performed using ANNOVAR (Wang et al., 2010). The gnomAD version 4.1 (Karczewski et al., 2020) and dbNSFP database (Liu et al., 2020) were used while performing the variant analysis.

Statistics

Statistical significance was determined by a Student's t-test and data are presented as means± SD.

Acknowledgments

We thank Christoph Seiler, Adele Donohue, and the Aquatics Facility team at Children's Hospital of Philadelphia for their excellent management of our zebrafish colonies and facilities. We also thank the CHOP Arcus team for provisioning computing infrastructure and virtual servers for data analysis, thank the Arcus Omics Science team for assistance in compiling exome sequencing files and clinical notes, and thank IDDRC Biostatistics and Data Science core (HD105354) for technical consultation. This work was supported by grants from the National Institutes of Health R01DE032332, Shriners Hospital for Children and Children's Hospital of Philadelphia Presidential Scholar Endowed Chair to ECL.

Competing interests

No competing interests declared

Funding sources

National Institutes of Health R01DE027983 supported this work to ECL, research support from Children's Hospital of Philadelphia, and research grants from the Shriners Hospitals for Children.

Data and resource availability

All relevant data and resource can be found within the article and its supplementary information.

References

Akin, M.A., Kurtoglu, S., Sarici, D., Akin, L., Hatipoglu, N., Korkmaz, L., Gunes, T., Ozturk, M.A., and Akcakus, M. (2014). Endocrine abnormalities of patients with cleft lip and/or cleft palate during the neonatal period. Turk J Med Sci *44*, 696-702.

Auer, T.O., Duroure, K., De Cian, A., Concordet, J.P., and Del Bene, F. (2014). Highly efficient CRISPR/Cas9-mediated knock-in in zebrafish by homology-independent DNA repair. Genome research *24*, 142-153.

Bebee, T.W., Park, J.W., Sheridan, K.I., Warzecha, C.C., Cieply, B.W., Rohacek, A.M., Xing, Y., and Carstens, R.P. (2015). The splicing regulators Esrp1 and Esrp2 direct an epithelial splicing program essential for mammalian development. eLife *4*.

Bowers, E.J., Mayro, R.F., Whitaker, L.A., Pasquariello, P.S., Larossa, D., and Randall, P. (1988). General body growth in children with cleft palate and related disorders: age differences. Am J Phys Anthropol *75*, 503-515.

Burguera, D., Marquez, Y., Racioppi, C., Permanyer, J., Torres-Mendez, A., Esposito, R., Albuixech-Crespo, B., Fanlo, L., D'Agostino, Y., Gohr, A.*, et al.* (2017). Evolutionary recruitment of flexible Esrp-dependent splicing programs into diverse embryonic morphogenetic processes. Nature communications *8*, 1799.

Caetano da Silva, C., Macias Trevino, C., Mitchell, J., Murali, H., Tsimbal, C., Dalessandro, E., Carroll, S.H., Kochhar, S., Curtis, S.W., Cheng, C.H.E.*, et al.* (2024). Functional analysis of ESRP1/2 gene variants and CTNND1 isoforms in orofacial cleft pathogenesis. Commun Biol *7*, 1040.

Camper, S.A., Smith, C., and Kitzman, J.O. (2023). Disruption of RNA Splicing Is an Important Contributor to Congenital Hypopituitarism and Other Human Genetic Diseases. Endocrinology *164*.

Carroll, S.H., Macias Trevino, C., Li, E.B., Kawasaki, K., Myers, N., Hallett, S.A., Alhazmi, N., Cotney, J., Carstens, R.P., and Liao, E.C. (2020). An Irf6-Esrp1/2 regulatory axis controls midface morphogenesis in vertebrates. Development *147*.

Cheung, L.Y., Davis, S.W., Brinkmeier, M.L., Camper, S.A., and Perez-Millan, M.I. (2017). Regulation of pituitary stem cells by epithelial to mesenchymal transition events and signaling pathways. Mol Cell Endocrinol *445*, 14-26.

Cox, L.L., Cox, T.C., Moreno Uribe, L.M., Zhu, Y., Richter, C.T., Nidey, N., Standley, J.M., Deng, M., Blue, E., Chong, J.X.*, et al.* (2018). Mutations in the Epithelial Cadherin-p120-Catenin Complex Cause Mendelian Non-Syndromic Cleft Lip with or without Cleft Palate. American journal of human genetics *102*, 1143-1157.

De Moerlooze, L., Spencer-Dene, B., Revest, J.M., Hajihosseini, M., Rosewell, I., and Dickson, C. (2000). An important role for the IIIb isoform of fibroblast growth factor receptor 2 (FGFR2) in mesenchymal-epithelial signalling during mouse organogenesis. Development *127*, 483-492.

de Moraes, D.C., Vaisman, M., Conceicao, F.L., and Ortiga-Carvalho, T.M. (2012). Pituitary development: a complex, temporal regulated process dependent on specific transcriptional factors. The Journal of endocrinology *215*, 239-245.

Derham, J.M., and Kalsotra, A. (2023). The discovery, function, and regulation of epithelial splicing regulatory proteins (ESRP) 1 and 2. Biochem Soc Trans *51*, 1097-1109.

Dixon, M.J., Marazita, M.L., Beaty, T.H., and Murray, J.C. (2011). Cleft lip and palate: understanding genetic and environmental influences. Nature reviews Genetics *12*, 167-178.
Dutta, S., Dietrich, J.E., Aspock, G., Burdine, R.D., Schier, A., Westerfield, M., and Varga, Z.M. (2005). pitx3 defines an equivalence domain for lens and anterior pituitary placode. Development *132*, 1579-1590.
Ericson, J., Norlin, S., Jessell, T.M., and Edlund, T. (1998). Integrated FGF and BMP signaling controls the progression of progenitor cell differentiation and the emergence of pattern in the embryonic anterior pituitary. Development *125*, 1005-1015.
Fabian, P., Tseng, K.C., Smeeton, J., Lancman, J.J., Dong, P.D.S., Cerny, R., and Crump, J.G. (2020). Lineage analysis reveals an endodermal contribution to the vertebrate pituitary. Science *370*, 463-467.
Fang, Q., George, A.S., Brinkmeier, M.L., Mortensen, A.H., Gergics, P., Cheung, L.Y., Daly, A.Z., Ajmal, A., Perez Millan, M.I., Ozel, A.B.*, et al.* (2016). Genetics of Combined Pituitary Hormone Deficiency: Roadmap into the Genome Era. Endocr Rev *37*, 636-675.
Glasgow, E., Karavanov, A.A., and Dawid, I.B. (1997). Neuronal and neuroendocrine expression of lim3, a LIM class homeobox gene, is altered in mutant zebrafish with axial signaling defects. Developmental biology *192*, 405-419.
Gregory, L.C., and Dattani, M.T. (2020). The Molecular Basis of Congenital Hypopituitarism and Related Disorders. J Clin Endocrinol Metab *105*.
Gross-Thebing, T., Paksa, A., and Raz, E. (2014). Simultaneous high-resolution detection of multiple transcripts combined with localization of proteins in whole-mount embryos. BMC biology *12*, 55.
Hawkins, M.B., Henke, K., and Harris, M.P. (2021). Latent developmental potential to form limb-like skeletal structures in zebrafish. Cell *184*, 899-911 e813.
Herzog, W., Sonntag, C., von der Hardt, S., Roehl, H.H., Varga, Z.M., and Hammerschmidt, M. (2004). Fgf3 signaling from the ventral diencephalon is required for early specification and subsequent survival of the zebrafish adenohypophysis. Development *131*, 3681-3692.
Herzog, W., Zeng, X., Lele, Z., Sonntag, C., Ting, J.W., Chang, C.Y., and Hammerschmidt, M. (2003). Adenohypophysis formation in the zebrafish and its dependence on sonic hedgehog. Developmental biology *254*, 36-49.
Higham, C.E., Johannsson, G., and Shalet, S.M. (2016). Hypopituitarism. Lancet *388*, 2403-2415.
Karczewski, K.J., Francioli, L.C., Tiao, G., Cummings, B.B., Alfoldi, J., Wang, Q., Collins, R.L., Laricchia, K.M., Ganna, A., Birnbaum, D.P.*, et al.* (2020). The mutational constraint spectrum quantified from variation in 141,456 humans. Nature *581*, 434-443.
Landrum, M.J., Lee, J.M., Riley, G.R., Jang, W., Rubinstein, W.S., Church, D.M., and Maglott, D.R. (2014). ClinVar: public archive of relationships among sequence variation and human phenotype. Nucleic acids research *42*, D980-985.
Laron, Z., Taube, E., and Kaplan, I. (1969). Pituitary growth hormone insufficiency associated with cleft lip and palate. An embryonal developmental defect. Helv Paediatr Acta *24*, 576-581.
Lee, S., Sears, M.J., Zhang, Z., Li, H., Salhab, I., Krebs, P., Xing, Y., Nah, H.D., Williams, T., and Carstens, R.P. (2020). Cleft lip and cleft palate in Esrp1 knockout mice is associated with alterations in epithelial-mesenchymal crosstalk. Development *147*.

Liu, X., Li, C., Mou, C., Dong, Y., and Tu, Y. (2020). dbNSFP v4: a comprehensive database of transcript-specific functional predictions and annotations for human nonsynonymous and splice-site SNVs. Genome Med *12*, 103.

McCabe, M.J., and Dattani, M.T. (2014). Genetic aspects of hypothalamic and pituitary gland development. Handb Clin Neurol *124*, 3-15.

Norlin, S., Nordstrom, U., and Edlund, T. (2000). Fibroblast growth factor signaling is required for the proliferation and patterning of progenitor cells in the developing anterior pituitary. Mechanisms of development *96*, 175-182.

Perez Millan, M.I., Cheung, L.Y.M., Mercogliano, F., Camilletti, M.A., Chirino Felker, G.T., Moro, L.N., Miriuka, S., Brinkmeier, M.L., and Camper, S.A. (2024). Pituitary stem cells: past, present and future perspectives. Nat Rev Endocrinol *20*, 77-92.

Pogoda, H.M., and Hammerschmidt, M. (2007). Molecular genetics of pituitary development in zebrafish. Seminars in cell & developmental biology *18*, 543-558.

Prodam, F., Caputo, M., Mele, C., Marzullo, P., and Aimaretti, G. (2021). Insights into non-classic and emerging causes of hypopituitarism. Nat Rev Endocrinol *17*, 114-129.

Rizzoti, K., and Lovell-Badge, R. (2005). Early development of the pituitary gland: induction and shaping of Rathke's pouch. Rev Endocr Metab Disord *6*, 161-172.

Rohacek, A.M., Bebee, T.W., Tilton, R.K., Radens, C.M., McDermott-Roe, C., Peart, N., Kaur, M., Zaykaner, M., Cieply, B., Musunuru, K., *et al.* (2017). ESRP1 Mutations Cause Hearing Loss due to Defects in Alternative Splicing that Disrupt Cochlear Development. Developmental cell *43*, 318-331 e315.

Roitman, A., and Laron, Z. (1978). Hypothalamo-pituitary hormone insufficiency associated with cleft lip and palate. Archives of disease in childhood *53*, 952-955.

Rudman, D., Davis, T., Priest, J.H., Patterson, J.H., Kutner, M.H., Heymsfield, S.B., and Bethel, R.A. (1978). Prevalence of growth hormone deficiency in children with cleft lip or palate. J Pediatr *93*, 378-382.

Takuma, N., Sheng, H.Z., Furuta, Y., Ward, J.M., Sharma, K., Hogan, B.L., Pfaff, S.L., Westphal, H., Kimura, S., and Mahon, K.A. (1998). Formation of Rathke's pouch requires dual induction from the diencephalon. Development *125*, 4835-4840.

Thisse, C., and Thisse, B. (2008). High-resolution in situ hybridization to whole-mount zebrafish embryos. Nature protocols *3*, 59-69.

Treier, M., Gleiberman, A.S., O'Connell, S.M., Szeto, D.P., McMahon, J.A., McMahon, A.P., and Rosenfeld, M.G. (1998). Multistep signaling requirements for pituitary organogenesis in vivo. Genes & development *12*, 1691-1704.

Wang, K., Li, M., and Hakonarson, H. (2010). ANNOVAR: functional annotation of genetic variants from high-throughput sequencing data. Nucleic acids research *38*, e164.

Warzecha, C.C., Jiang, P., Amirikian, K., Dittmar, K.A., Lu, H., Shen, S., Guo, W., Xing, Y., and Carstens, R.P. (2010). An ESRP-regulated splicing programme is abrogated during the epithelial-mesenchymal transition. The EMBO journal *29*, 3286-3300.

Yang, Y., Park, J.W., Bebee, T.W., Warzecha, C.C., Guo, Y., Shang, X., Xing, Y., and Carstens, R.P. (2016). Determination of a Comprehensive Alternative Splicing Regulatory Network and Combinatorial Regulation by Key Factors during the Epithelial-to-Mesenchymal Transition. Molecular and cellular biology *36*, 1704-1719.

Zhu, X., Gleiberman, A.S., and Rosenfeld, M.G. (2007). Molecular physiology of pituitary development: signaling and transcriptional networks. Physiol Rev *87*, 933-963.
Zilinski, C.A., Shah, R., Lane, M.E., and Jamrich, M. (2005). Modulation of zebrafish pitx3 expression in the primordia of the pituitary, lens, olfactory epithelium and cranial ganglia by hedgehog and nodal signaling. Genesis *41*, 33-40.

Figure Legends

Fig. 1. *Esrp1 and Esrp2* are expressed in the developing mouse anterior pituitary. Sagittal sections of wildtype mouse Rathke's pouch at E10.25 (**A**), E11.5 (**B**), and E12.5 (**C**) analyzed by RNAscope *in situ* hybridization. Embryos are oriented with rostral to the left and dorsal at the top. Images to left are low magnification while images to right are higher magnification of boxed area. Staining shows cellular co-expression of *Esrp1* (red) and *Esrp2* (white) in the invaginating oral epithelium and in the developing Rathke's pouch (A and B). C) *Esrp1* and *Esrp2* expression persist after the closure of Rathke's pouch. **D**) *Esrp1* and *Esrp2* continue to be expressed in the anterior and intermediate pituitary gland of mice at birth (P0). N=3. Scale bar = 100 μm.

Fig. 2. *Esrp1-/-,Esrp2-/-* null mice have an absent or severely hypoplastic anterior pituitary. **A**) Coronal H&E stained sections of P0 littermate control (*Esrp1* +/+, *Esrp2* +/-) and *Esrp1-/-, Esrp2-/-* null pituitary. The top row shows a rostral-positioned section, the middle row shows an enlargement of the boxed area, and the bottom row shows a caudal-positioned section. *Esrp1-/-,Esrp2-/-* null mice have a severely hypoplastic or absent anterior pituitary. The intermediate pituitary is somewhat intact while the posterior pituitary appears unaffected. **B**) Coronal sections of E17.5 littermate control (*Esrp1* +/+, *Esrp2* +/-) and *Esrp1-/-,Esrp2-/-* null pituitary immunostained for Sox2 (magenta), growth hormone (GH, green) or POMC (magenta). Remnant pituitary tissue of *Esrp1-/-,Esrp2-/-* null mice highly expresses the pituitary stem cell marker Sox2,

similar to the expression in the control intermediate pituitary, however, no GH expression and minimal POMC expression was detected. N=3. Scale bar = 100 μm.

Fig. 3. *Esrp1-/-,Esrp2-/-* null mice have impaired Rathke's pouch formation. Sagittal sections of Rathke's pouch in E12.5 littermate control (*Esrp1* +/+, *Esrp2* +/-) and two individual *Esrp1-/-, Esrp2-/-* null mouse embryos. **A**) H&E staining shows Rathke's pouch of *Esrp1-/-, Esrp2-/-* null embryos to be significantly smaller and dysmorphic relative to controls. N=3 Scale = 100 μm. **B)** RNAscope *in situ* hybridization showing *Sox2* (green), *Lhx3* (white), and *Prop1* (red) expression. Expression is similar in control and *Esrp1-/-,Esrp2-/-* null embryos despite Rathke's pouch being hypoplastic and dysmorphic in the nulls. N=3. Scale = 100 μm.

Fig. 4. *Esrp1-/-,Esrp2-/-* null mice express less *Fgfr1IIIb* isoform within the invaginating Rathke's pouch. Sagittal sections and Basescope *in situ* hybridiation of Rathke's pouch in E10.5 littermate control (*Esrp1* +/+, *Esrp2* +/+) and *Esrp1-/-, Esrp2-/-* null mouse embryos. **A**) Representative images showing Rathke's pouch where *in situ* hybridization was performed for *Fgfr1IIIb* (green) and *Fgfr1IIIc* (red) isoforms. Magnification of boxed area where staining for *Fgfr1IIIb* transcripts is indicated by arrowheads. Scale = 10 μm. **B)** Quantification of the number of *Fgfr1* isoform transcripts normalized to the total number of cells within Rathke's pouch. N=3.

Fig. 5. Zebrafish ADH placode and developing ADH express *esrp1*. Midline sagittal sections of wildtype zebrafish embryo at 24 hpf **A**) and 27 hpf **B**), analyzed by

RNAscope *in situ* hybridization. Embryos are oriented with rostral to the left and dorsal at the top. Images to the right are increased magnifications of the boxed area to the left. **A**) At 24 hpf, *esrp1* (red) is expressed in the ADH placode, which was identified by *pitx3* (cyan) expression. **B**) At the time of posterior migration (27 hpf), *esrp1* is expressed in the developing ADH, identified by *pomca* expression (yellow). *esrp1* expression is also expressed in the developing oral epithelium. N=2. Scale bar = 50 μm.

Fig. 6. *esrp1-/-,esrp2-/-* mutant zebrafish display ADH dysmorphogenesis. A) Whole-mount *in situ* hybridization of 3 dpf clutch-mate control and *esrp1-/-,esrp2-/-* mutant zebrafish. *pomca*, *prolactin* (*prl*), and *growth hormone* (*gh*) expression are displaced ventrally and rostrally in the *esrp1-/-,esrp2-/-* mutants relative to controls. Further, *pomca* expression is detected in the oral epithelium (arrow) of *esrp1-/-,esrp2-/-* mutants. N=5. **B**) Dorsal view of 3D reconstruction of confocal imaging of *pomca* whole-mount RNAscope *in situ* hybridization of clutch-mate control and *esrp1-/-,esrp2-/-* mutant zebrafish at 3 dpf. While expression of *pomca* (magenta) in the control animals was observed as expected, *pomca* expression in *esrp1-/-,esrp2-/-* mutants was detected in a more ventral position and extended into the oral epithelium (arrows). N=2 **C**) RNAscope *in situ* hybridization of midline sagittal sections of clutch-mate control and *esrp1-/-,esrp2-/-* mutant 3 dpf zebrafish. In controls, ADH markers *lhx3* (red), *pitx3* (cyan), *prl* (yellow), and *pomca* (magenta) are expressed as expected caudal to the ethmoid plate and adjacent to the hypothalamus. In *esrp1-/-,esrp2-/-* mutants, *lhx3*, *pitx3*, *prl,* and *pomca* are expressed within the oral cavity, highly rostral to normal positioning. Further, *pomca* expression in *esrp1-/-,esrp2-/-* mutants is normal within the

hypothalamus but also more widespread than the other ADH genes. *krt4* expression was also detected (green) to identify oral epithelium. N=2,3. Scale bar = 100 μm.

Fig. 7. An lhx3:tdTomato reporter line shows impaired ADH anlage translocation in *esrp1-/-,esrp2-/-* mutant zebrafish. A) Schematic illustrating the generation of a zebrafish pituitary reporter line. **B-E)** Light-sheet microscopy (LSM) imaging of zebrafish expressing *lhx3*:tdTomato (magenta) and *cdh1*:gfp (gray). **B)** Frontal snapshots of LSM *in vivo* imaging from 27 to 42 hpf. **C)** Snapshots of sagittal optical sections of LSM in vivo imaging from B. **D)** Frontal and sagittal optical sections of LSM generated images of clutch-mate control and *esrp1-/-, esrp2-/-* zebrafish at 48 hpf. Dotted line delineates embryo surface and oral opening. **E)** LSM-generated optical section through ventral view of *esrp1-/-, esrp2-/-* zebrafish at 72 hpf. Dotted line delineates the eyes (E) and the anterior neurocranium cartilage (ANC). N=3. Scale bar = 50 μm.

Fig. 8. A deleterious *ESRP2* variant in a patient with hypopituitarism and cleft palate. A) A schematic of the human *ESRP2* gene. The red asterisk represents the location of the SNV identified in a hypopituitarism and cleft palate patient. **B)** Schematic of Esrp2 protein domains. The red asterisk represents the location of the resulting amino acid change within the RNA binding domain (RBD) of Esrp2. The blue asterisks represent the locations of previously identified *ESRP2* variants associated with cleft palate (Cox et al., 2018). **C)** *ESRP2* amino acid sequences compared across species. The boxed region identifies the conserved arginine residue that is affected by the SNV.

Fig. S1. ***Esrp1-/-,Esrp2-/-* and *Esrp1-/-,Esrp2*+/+ mice have an absent or severely hypoplastic anterior pituitary.** **A**) Coronal H&E stained sections of E17.5 littermate control (*Esrp1* +/+, *Esrp2* +/-) and *Esrp1-/-, Esrp2-/-* null pituitary. Two control and 2 null embryos are shown. N=2. **B**) Coronal H&E stained sections of E17.5 littermate control (*Esrp1* +/+, *Esrp2* +/+) and *Esrp1-/-,Esrp2*+/+ pituitary. N=1. Scale bar = 100 μm.

Fig. S2. *Esrp1-/-,Esrp2-/-* null mice have impaired Rathke's pouch formation. Sagittal sections of Rathke's pouch in three E12.5 littermate controls and two *Esrp1-/-, Esrp2-/-* null mouse embryos. **A**) H&E staining shows Rathke's pouch of *Esrp1-/-, Esrp2-/-* null embryos to be significantly smaller and dysmorphic relative to controls. Scale bar = 0.1 mm. **B**) Increased magnification of Rathke's pouch. Scale bar = 100 μm.

Movie 1. Frontal view light-sheet microscopy (LSM) imaging of 27 hpf zebrafish expressing *lhx3*:tdTomato (magenta) and *cdh1*:gfp (gray). Images were collected every 15 minutes for 15 hours.

Movie 2. Medial sagittal optical section of lateral view light-sheet microscopy (LSM) imaging of 27 hpf zebrafish expressing *lhx3*:tdTomato (magenta) and *cdh1*:gfp (gray). Images were collected every 15 minutes for 15 hours.

Movie 3. Frontal view light-sheet microscopy (LSM) imaging of 27 hpf zebrafish from Movie 1 with only *cdh1*:gfp (gray) expression displayed.

Movie 4. Medial sagittal optical section of lateral view light-sheet microscopy (LSM) imaging of 27 hpf zebrafish from Movie 2 with only *cdh1*:gfp (gray) expression displayed.

Figure 1

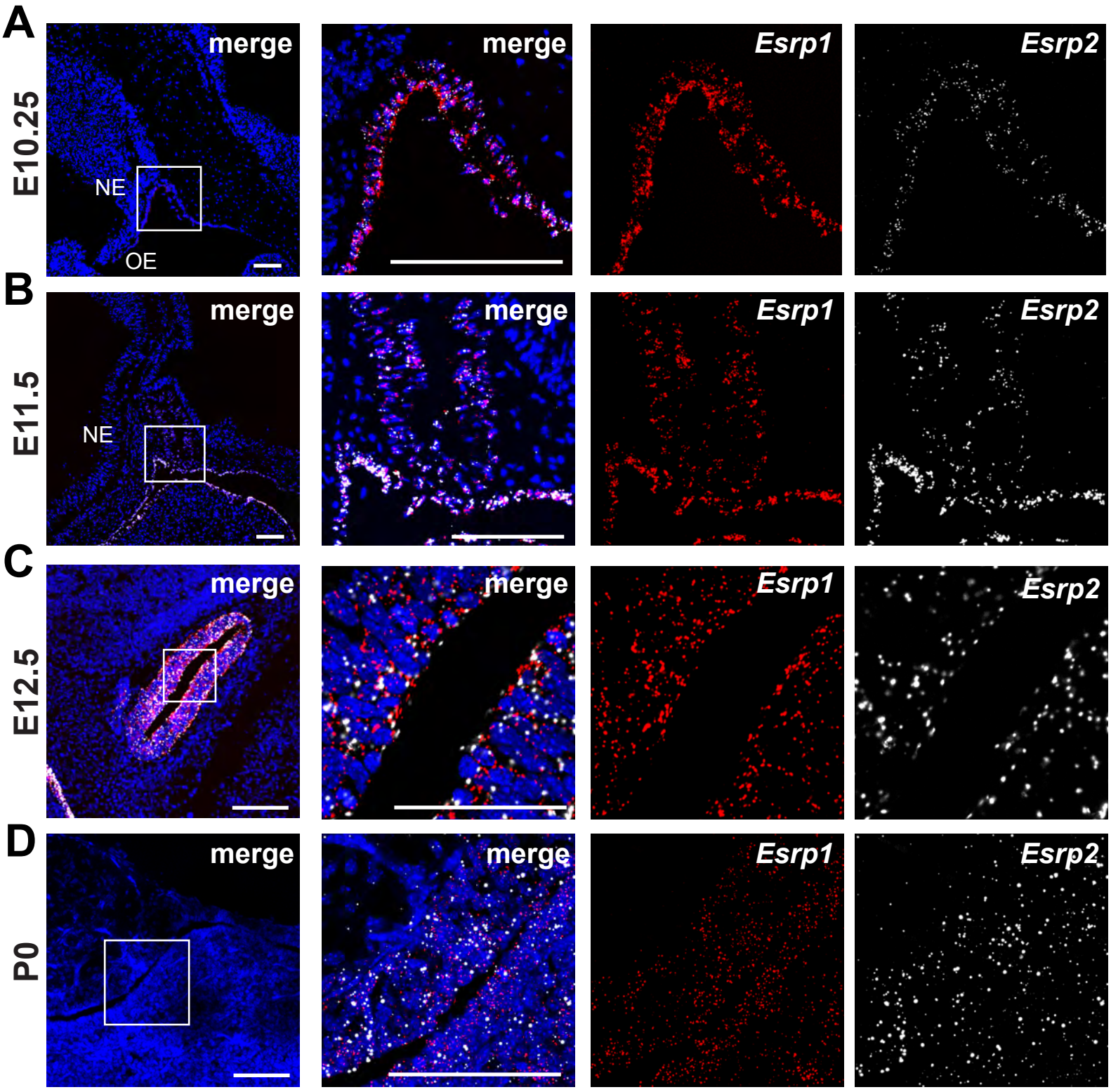

Figure 2

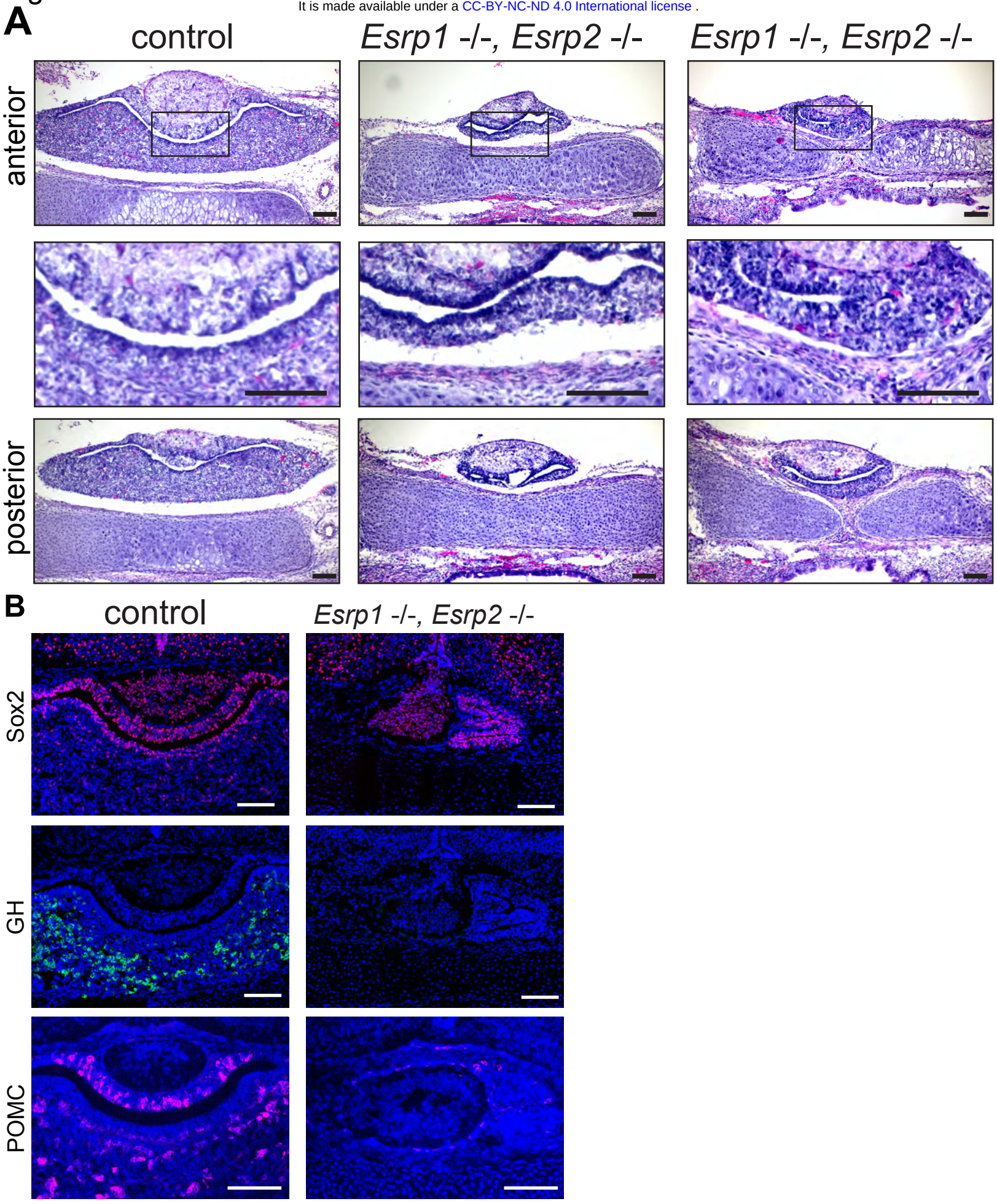

Figure 3

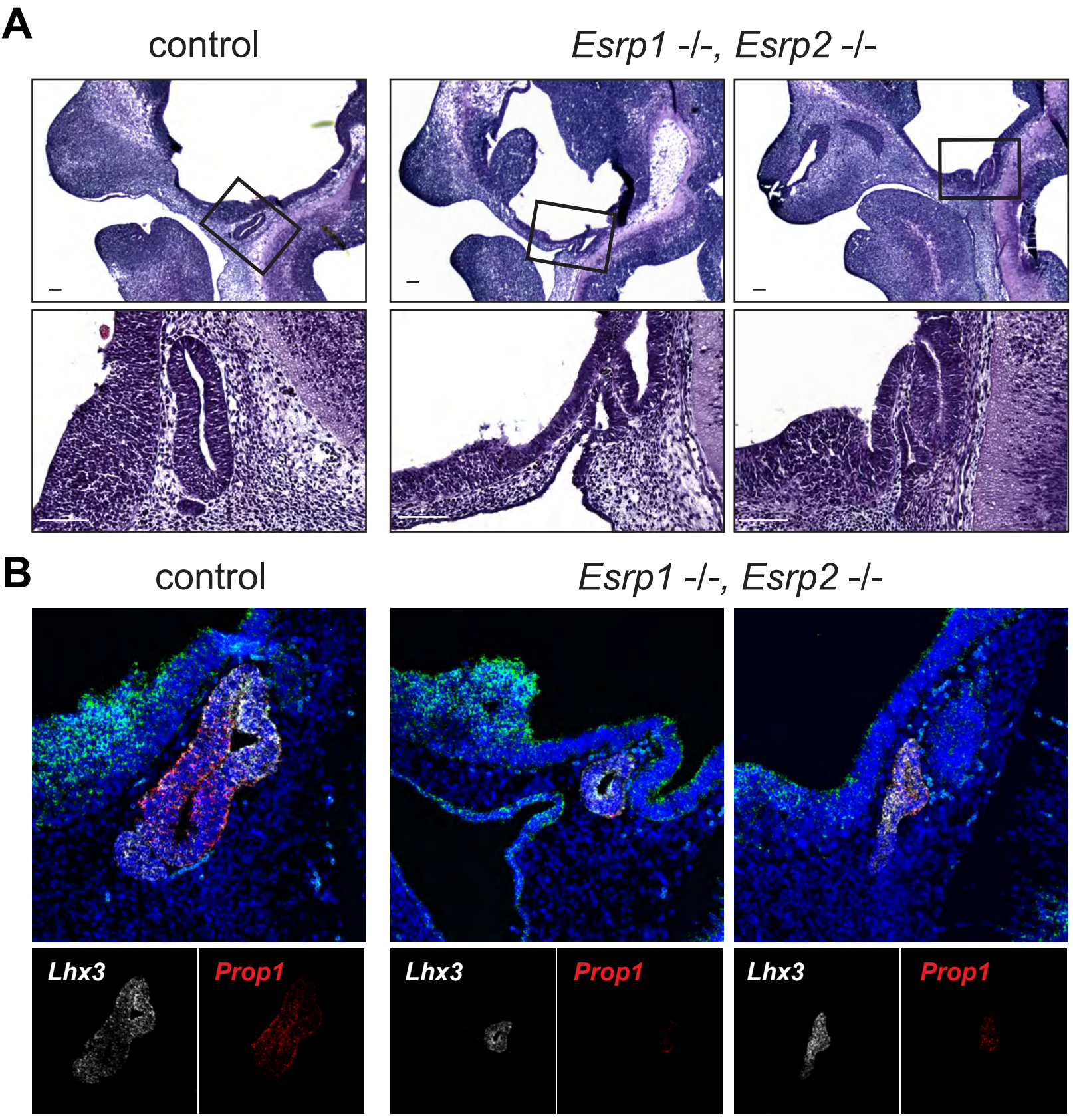

Figure 4

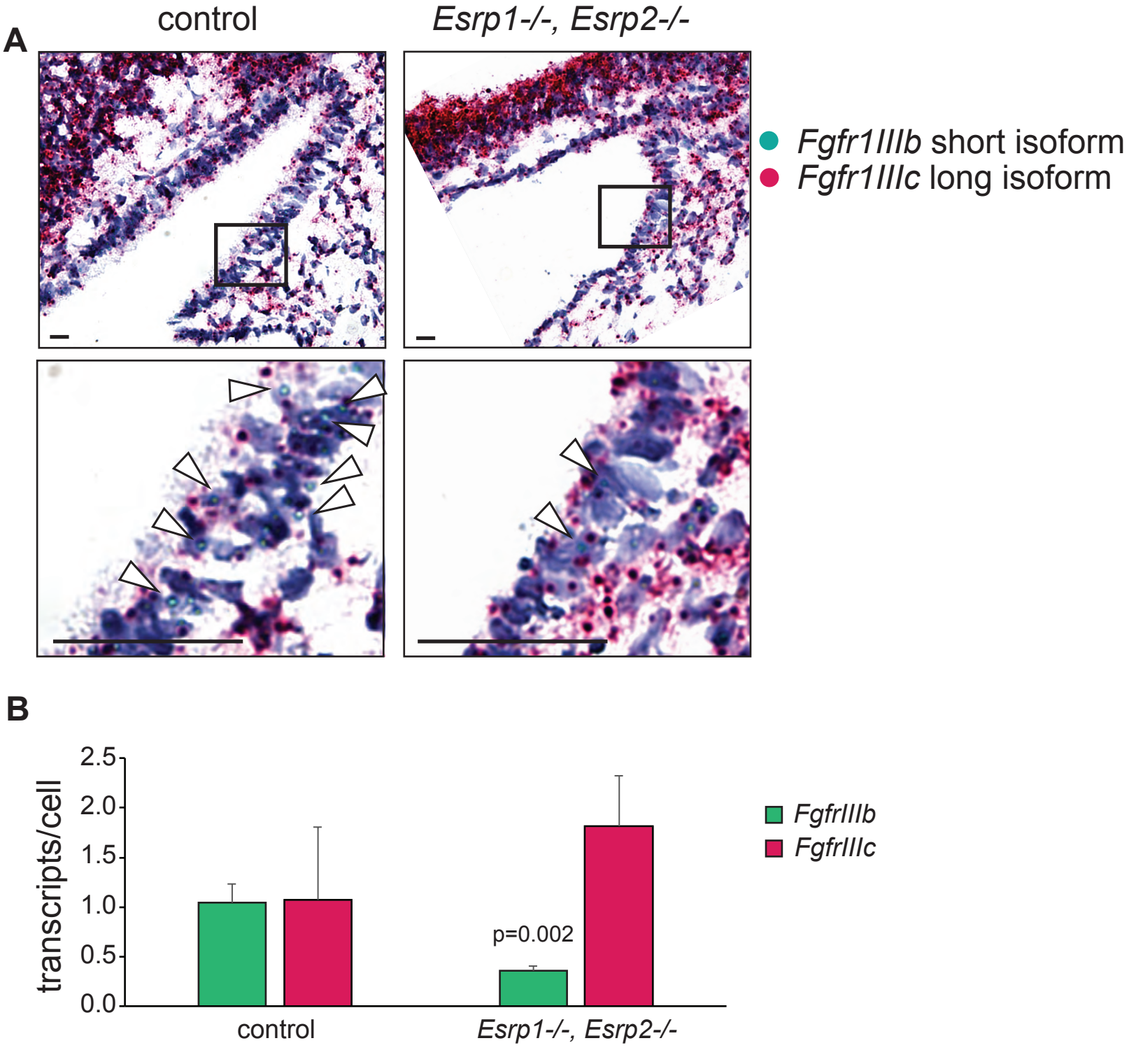

Figure 5

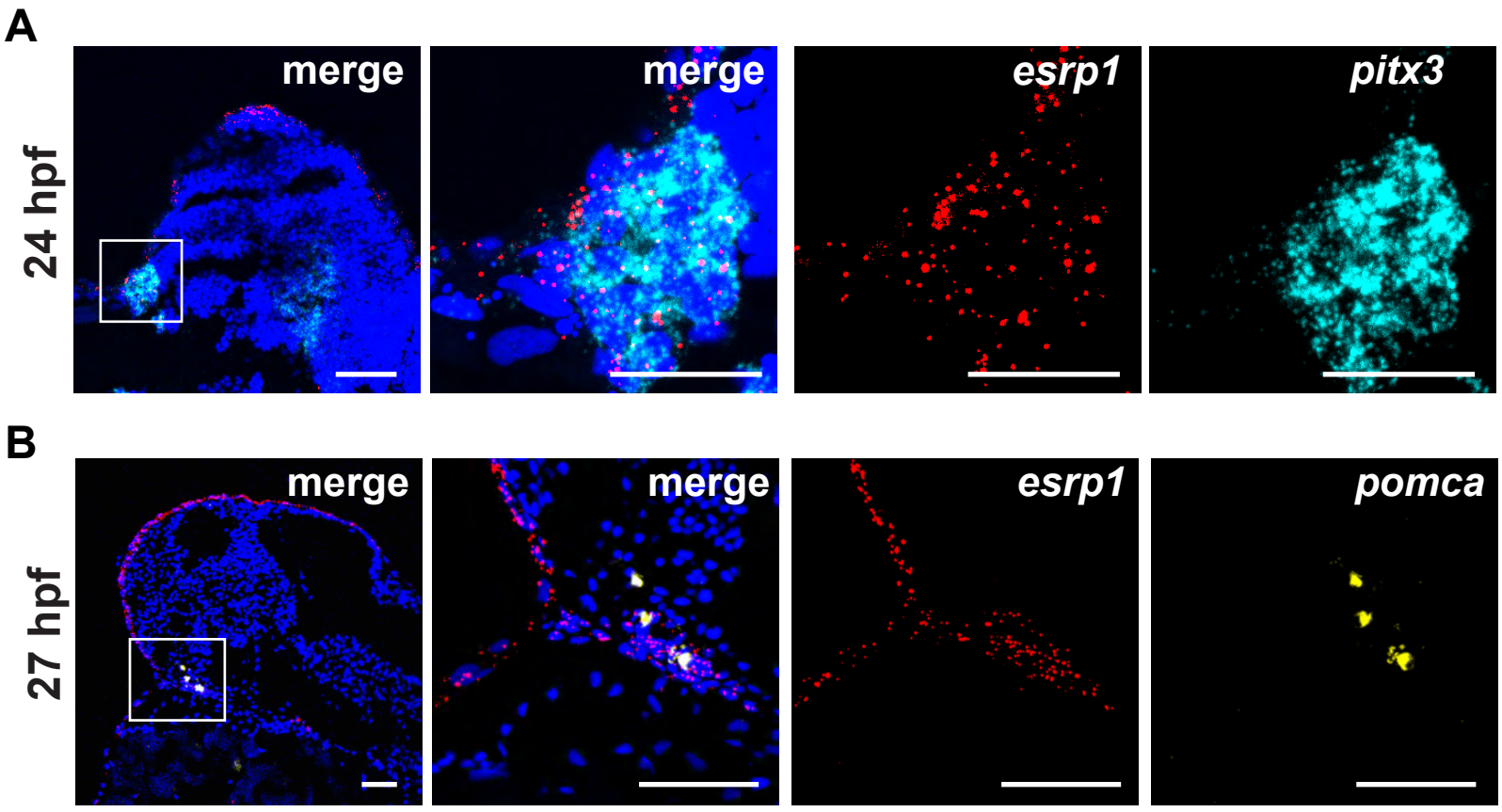

Figure 6

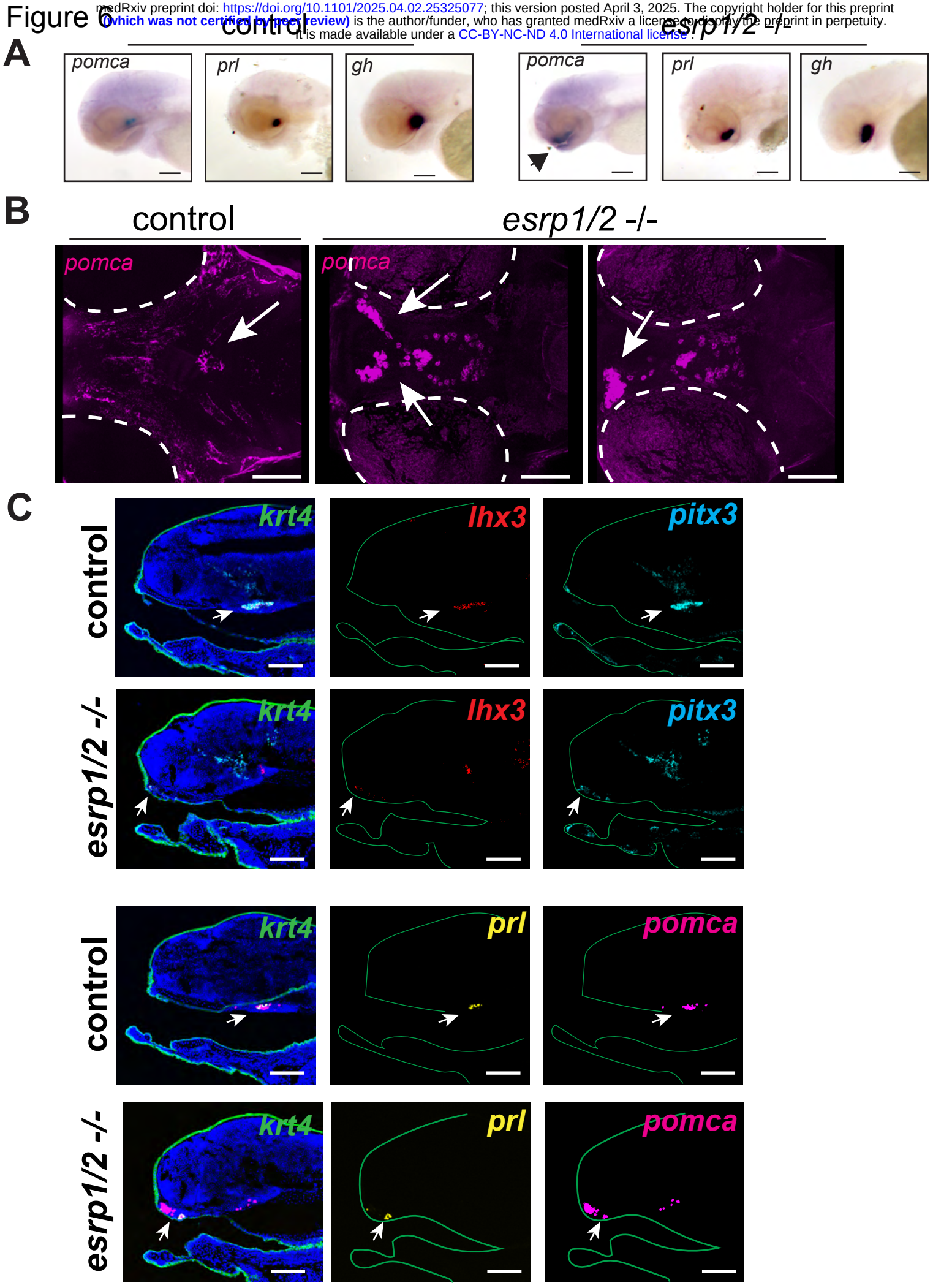

Figure 7

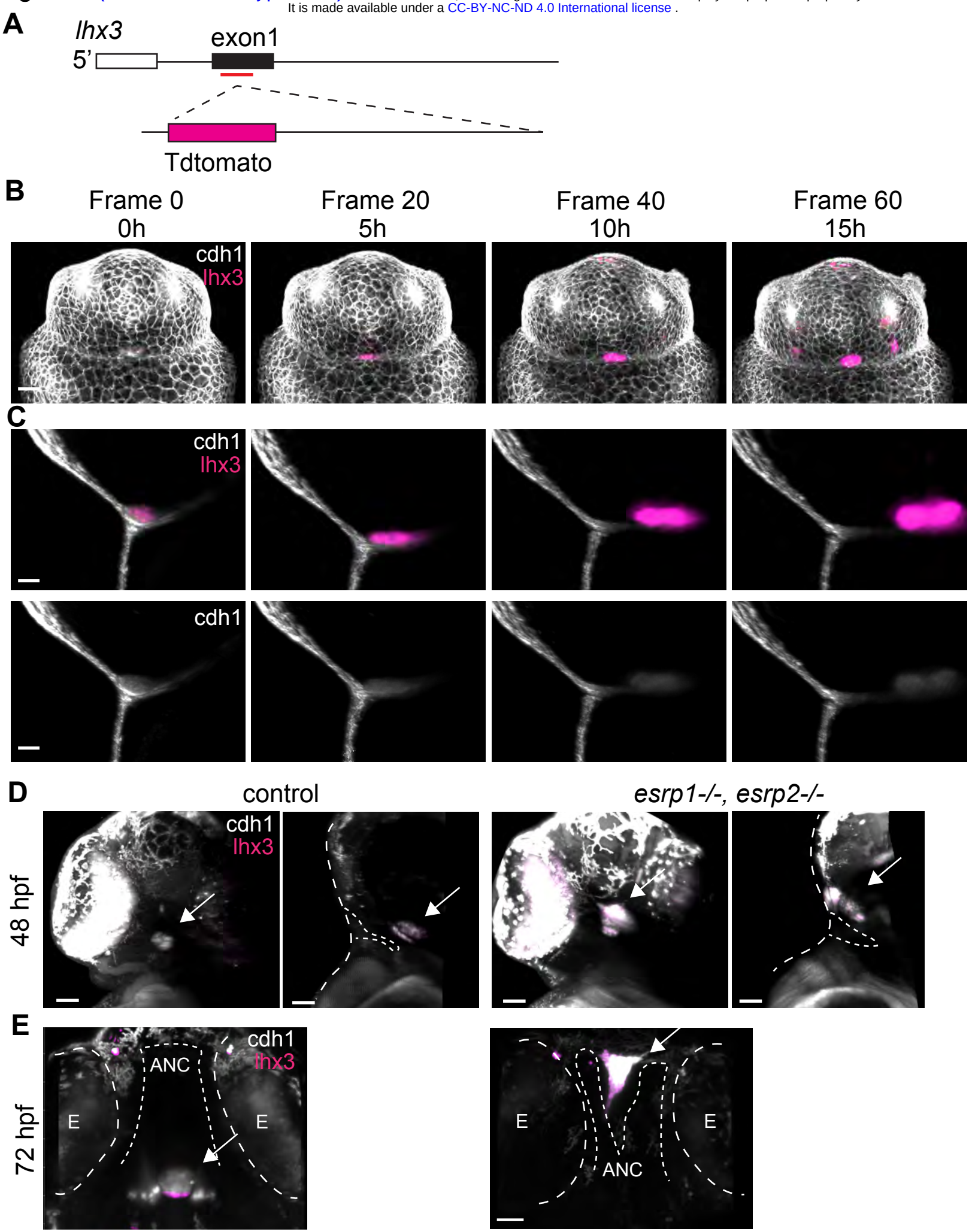

Figure 8